

# Proximal MCMC for Bayesian Inference of Constrained and Regularized Estimation

Xinkai Zhou\*      Eric C. Chi†      Hua Zhou‡

## Abstract

This paper advocates proximal Markov Chain Monte Carlo (ProxMCMC) as a flexible and general Bayesian inference framework for constrained or regularized estimation. Originally introduced in the Bayesian imaging literature, ProxMCMC employs the Moreau-Yosida envelope for a smooth approximation of the total-variation regularization term, fixes nuisance and regularization parameters as constants, and relies on the Langevin algorithm for the posterior sampling. We extend ProxMCMC to the full Bayesian framework with modeling and data adaptive estimation of all parameters including the regularization strength parameter. More efficient sampling algorithms such as the Hamiltonian Monte Carlo are employed to scale ProxMCMC to high-dimensional problems. Analogous to the proximal algorithms in optimization, ProxMCMC offers a versatile and modularized procedure for the inference of constrained and non-smooth problems. The power of ProxMCMC is illustrated on various statistical estimation and machine learning tasks. The inference in these problems is traditionally considered difficult from both frequentist and Bayesian perspectives.

**Keywords:** Credible interval, regularization, constraints, Moreau-Yosida envelope, proximal mapping, MCMC, Hamiltonian Monte Carlo

## 1 Introduction

Many statistical learning tasks are posed as penalized maximum likelihood estimation problems, which require solving optimization problems of the form

$$\text{maximize } \ell(\boldsymbol{\theta}) - \rho g(\boldsymbol{\theta}),$$

where  $\boldsymbol{\theta}$  is a parameter specifying a model,  $\ell(\boldsymbol{\theta})$  is a log-likelihood quantifying lack-of-fit between the model parameterized by  $\boldsymbol{\theta}$  and the data,  $g(\boldsymbol{\theta})$  is a penalty function that promotes the recovery of parameter estimates that have a desired structure, and  $\rho$  is a nonnegative regularization strength parameter that trades off model fit encoded in  $\ell(\boldsymbol{\theta})$  with the desired structure encoded in  $g(\boldsymbol{\theta})$ . Canonical examples of penalty functions for  $g(\boldsymbol{\theta})$  include the  $\ell_1$ -norm which incentivizes recovery of

---

\*Department of Biostatistics, UCLA, Los Angeles, CA, USA, Email: xinkaizhou@ucla.edu

†Department of Statistics, Rice University, Houston, TX, USA, Email: echi@rice.edu

‡Department of Biostatistics, UCLA, Los Angeles, CA, USA, Email: huazhou@ucla.edu

sparse models and the nuclear norm which incentivizes recovery of low-rank models. To date, most work has focused exclusively on point estimates without quantifying the uncertainty in the estimates. Lacking tools for assessing the uncertainty in findings from regularized models, practitioners often resort to classical inference tools designed for fixed models. This practice can lead to seriously inflated type I error and is partly to blame for the reproducibility crisis in science (Ioannidis, 2005).

This challenge has motivated the development of post-selection inference techniques such as simultaneous inference (Berk et al., 2013; Bachoc et al., 2020; Kuchibhotla et al., 2020) and selective inference (Lee et al., 2016; Choi et al., 2017; Taylor and Tibshirani, 2018). A closely related approach calculates confidence intervals for coefficients of high-dimensional linear models through bias-correction (van de Geer et al., 2014; Zhang and Zhang, 2014; Javanmard and Montanari, 2014). Most of this literature, however, focuses on variable selection through the  $\ell_1$ -penalty. Extending these strategies to more complicated penalties and constraints is not straightforward. Moreover, caution is warranted when reporting these confidence intervals because their interpretation (e.g., conditional on the selection event) can be quite different from traditional ones.

An alternative approach is to cast the problem in the Bayesian framework. For example, Park and Casella (2008) introduced the Bayesian lasso. In this work, the  $\ell_1$ -penalty was identified with a Laplace prior and a Gibbs sampler was used to sample from the posterior distribution. This early work helped spark the development of Bayesian variable selection methods, specifically alternative sparsity inducing prior distributions such as the spike-and-slab prior (Mitchell and Beauchamp, 1988; George and McCulloch, 1993), horseshoe prior (Carvalho et al., 2010; Polson and Scott, 2010; Pironen and Vehtari, 2017), the orthant normal prior (Hans, 2011), the correlated Normal-Gamma prior (Griffin and Brown, 2012, 2013), the generalized double Pareto prior (Armagan et al., 2013), and the Dirichlet-Laplace prior (Bhattacharya et al., 2015). While there have been many innovations in Bayesian techniques for variable selection, more general penalties and constraints beyond sparsity require substantially more problem-specific analysis.

More recently, Pereyra (2016) and Durmus et al. (2018) proposed the proximal Markov Chain Monte Carlo (ProxMCMC) algorithm for quantifying uncertainty in Bayesian imaging applications where the penalties of interest include the total-variation semi-norm (Rudin et al., 1992) and the  $\ell_1$ -norm. To deal with the non-smoothness of these penalties, they employ the Moreau-Yosida envelope to obtain a smooth approximation to the total-variation semi-norm and  $\ell_1$ -norm penalties. Samples from the smooth approximate posterior distribution can be generated via the Langevin algorithm.

Their proposed approach opens the door to a potentially general and flexible framework for performing posterior inference for penalized regression models whenever the penalty term is convex and admits a proximal map which can be computed easily – a situation that holds true for a wide variety of convex penalties. The fly in the ointment, however, is that their approach requires manually setting the regularization strength parameter  $\rho$ . This limitation prevents the previous formulations of ProxMCMC from being a fully Bayesian framework for generating posterior samples for many existing and more importantly potentially yet-to-be-invented non-smooth penalties.

**Contributions:** In this paper, we address this limitation and extend ProxMCMC to be fully Bayesian by incorporating penalties and constraints through epigraph priors. Our extended Prox-

MCMC inference framework is suitable for regularized or constrained statistical learning problems and offers three main advantages.

First, it provides valid and automatic statistical inference even for problems that involve non-smooth and potentially non-convex penalties or constraints. The inference for such problems is traditionally considered difficult.

Second, it is fully Bayesian so that parameter tuning is not required, in contrast to previous ProxMCMC methods (Durmus et al., 2018) where the regularization strength parameters are either manually fixed or needs to be tuned.

Third, the method is highly modular in the sense that its components – model, prior, proximal map, and sampling algorithm – are independent of each other and thus can be modified to accommodate new problems. This feature makes ProxMCMC easily customizable so that practitioners can adapt it to their unique problems. For example, in analyzing compositional data from microbiome studies, one often needs to fit a lasso model where regression coefficients sum to 0. Although such problems are difficult to tackle in a post-selection inference framework, as we will demonstrate later in Section 5.1, it is straightforward to solve using our ProxMCMC method.

Finally, we put our ProxMCMC method on firm foundations by providing guarantees on properness of the approximate posterior and show that the approximate posterior can be made arbitrarily close to a target posterior in total-variation for both convex and non-convex penalties and constraints.

The rest of our paper is organized as follows. Section 2 reviews concepts from convex optimization that underlie the algorithmic building blocks of our ProxMCMC framework. Section 3 illustrates our method using the familiar lasso problem. Section 4 summarizes the key elements from our case study of the lasso to show how our ProxMCMC method can be applied generally. Section 5 presents a variety of illustrative applications. Sections 6 and 7 provide theoretical guarantees and discussions respectively.

## 2 Background

We review concepts from convex analysis essential for ProxMCMC, specifically Moreau-Yosida envelopes and proximal maps. For a more thorough review of proximal maps and their applications in statistics and machine learning, we refer readers to (Combettes and Wajs, 2005; Combettes and Pesquet, 2011; Polson et al., 2015). Recall in convex optimization it is often convenient to work with functions that map into the extended reals,  $\bar{\mathbb{R}} = \mathbb{R} \cup \{\infty\}$ . The indicator function of a set  $C$ , denoted  $\delta_C(\mathbf{x})$ , is the function that is zero for all  $\mathbf{x} \in C$  and is infinity for all  $\mathbf{x} \notin C$ . When the set  $C$  is closed and convex, the indicator function  $\delta_C(\mathbf{x})$  of  $C$  is lower-semicontinuous and convex. A function  $g$  is proper if it takes on a finite value for some element in its domain. Let  $\Gamma(\mathbb{R}^m)$  denote the set of all proper, lower-semicontinuous, convex functions from  $\mathbb{R}^m$  into  $\bar{\mathbb{R}}$ . Let  $\|\mathbf{x}\|$  denote the Euclidean norm of a point  $\mathbf{x}$ .

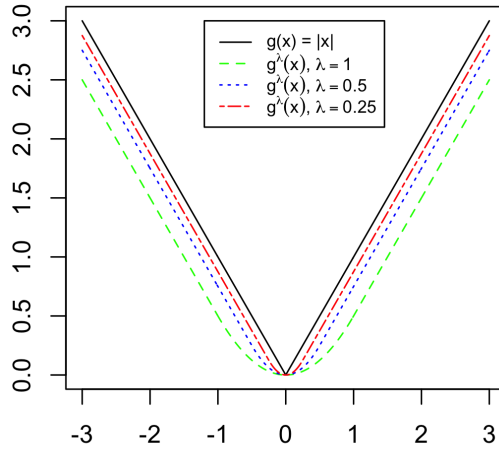


Figure 1: The Moreau-Yosida envelope of the absolute value function  $g(x) = |x|$ .

## 2.1 Moreau-Yosida Envelopes and Proximal Maps

**Definition 1.** Given  $g \in \Gamma(\mathbb{R}^m)$  and a positive scaling parameter  $\lambda$ , the Moreau-Yosida envelope of  $g$ , denoted by  $g^\lambda$ , is given by

$$g^\lambda(\mathbf{x}) = \inf_{\boldsymbol{\omega}} \left\{ g(\boldsymbol{\omega}) + \frac{1}{2\lambda} \|\boldsymbol{\omega} - \mathbf{x}\|^2 \right\}.$$

The infimum is always attained at a unique point when  $g \in \Gamma(\mathbb{R}^m)$ , and the minimizer defines the proximal map of  $g$ .

**Definition 2.** Given  $g \in \Gamma(\mathbb{R}^m)$  and a positive scaling parameter  $\lambda$ , the proximal map of  $g$ , denoted  $\text{prox}_g^\lambda$ , is given by

$$\text{prox}_g^\lambda(\mathbf{x}) = \arg \min_{\boldsymbol{\omega}} \left\{ g(\boldsymbol{\omega}) + \frac{1}{2\lambda} \|\boldsymbol{\omega} - \mathbf{x}\|^2 \right\}.$$

The well known Huber function (Beck, 2017, Example 6.54)

$$g^\lambda(x) = \begin{cases} \frac{1}{2\lambda} x^2 & \text{if } |x| \leq \lambda \\ |x| - \frac{\lambda}{2} & \text{otherwise} \end{cases}$$

is the Moreau-Yosida envelope of the absolute value function  $g(x) = |x|$ . Figure 1 shows  $g(x)$  and  $g^\lambda(x)$  for three different  $\lambda$  values. We can see immediately from this familiar example from robust statistics that the Moreau-Yosida envelope provides a differentiable approximation to a non-smooth function where the approximation improves as  $\lambda$  gets smaller.

In general, the Moreau-Yosida envelope  $g^\lambda(\mathbf{x})$  has several important properties. First,  $g^\lambda(\mathbf{x})$  is convex when  $g(\mathbf{x})$  is convex. Second, if  $g(\mathbf{x})$  is convex, then  $g^\lambda(\mathbf{x})$  is always differentiable even if  $g(\mathbf{x})$  is not, and its gradient can be expressed in terms of  $\text{prox}_g^\lambda(\mathbf{x})$ , namely

$$\nabla g^\lambda(\mathbf{x}) = \frac{1}{\lambda} [\mathbf{x} - \text{prox}_g^\lambda(\mathbf{x})]. \quad (1)$$

Moreover,  $\nabla g^\lambda(\mathbf{x})$  is  $\lambda^{-1}$ -Lipschitz since proximal operators are firmly nonexpansive (Combettes and Pesquet, 2011). Finally and most importantly,  $g^\lambda(\mathbf{x})$  converges pointwise to  $g(\mathbf{x})$  as  $\lambda$  tends to zero (Rockafellar and Wets, 2009). In summary, the Moreau-Yosida envelope of a non-smooth function  $g(\mathbf{x})$  is a Lipschitz-differentiable, arbitrarily close approximation to  $g(\mathbf{x})$ .

The closely related proximal maps play a prominent role in modern statistical learning since many popular non-smooth penalties have unique proximal maps that either have explicit formulas or can be computed efficiently. For example, the proximal map of  $g(\mathbf{x}) = \|\mathbf{x}\|_1$  is the celebrated soft-thresholding operator  $S_\lambda(\mathbf{x})$  defined by

$$S_\lambda(\mathbf{x})_i = \begin{cases} x_i - \lambda & \text{if } x_i > \lambda \\ 0 & \text{if } |x_i| \leq \lambda \\ x_i + \lambda & \text{if } x_i < -\lambda. \end{cases} \quad (2)$$

When the function  $g$  is an indicator function  $\delta_{\mathcal{E}}$  of a set  $\mathcal{E}$ , the proximal map  $\text{prox}_{\delta_{\mathcal{E}}}^\lambda(\mathbf{x})$  is the Euclidean projection operator onto the set  $\mathcal{E}$ , namely

$$\mathcal{P}_{\mathcal{E}}(\mathbf{x}) = \arg \min_{\boldsymbol{\omega} \in \mathcal{E}} \|\boldsymbol{\omega} - \mathbf{x}\|$$

for all  $\lambda > 0$ . Let  $d_{\mathcal{E}}(\mathbf{x})$  denote the Euclidean distance of the point  $\mathbf{x}$  to the set  $\mathcal{E}$ , namely

$$d_{\mathcal{E}}(\mathbf{x}) = \inf_{\mathbf{y} \in \mathcal{E}} \|\mathbf{x} - \mathbf{y}\|,$$

then  $\mathcal{P}_{\mathcal{E}}(\mathbf{x})$  is the point in  $\mathcal{E}$  that is closest in Euclidean distance to the set  $\mathbf{x}$ , namely

$$d_{\mathcal{E}}(\mathbf{x}) = \|\mathbf{x} - \mathcal{P}_{\mathcal{E}}(\mathbf{x})\|,$$

and the Moreau-Yosida envelope  $g^\lambda(\mathbf{x})$  of  $g(\mathbf{x}) = \delta_{\mathcal{E}}(\mathbf{x})$  is

$$g^\lambda(\mathbf{x}) = \frac{1}{2\lambda} d_{\mathcal{E}}^2(\mathbf{x}) = \frac{1}{2\lambda} \|\mathbf{x} - \mathcal{P}_{\mathcal{E}}(\mathbf{x})\|^2.$$

## 2.2 Projections onto Epigraphs

The key algorithmic primitive in our ProxMCMC framework is the projection onto the epigraph of a penalty function  $g(\mathbf{x})$ , namely the set

$$\mathcal{E} = \text{epi}(g) = \{(\mathbf{x}, \alpha) : g(\mathbf{x}) \leq \alpha\}.$$

The Moreau-Yosida envelope of the indicator function  $g(\mathbf{x}, \alpha) = \delta_{\mathcal{E}}(\mathbf{x}, \alpha)$  of  $\mathcal{E} = \text{epi}(g)$  plays a central role in defining our Bayesian hierarchical model. The Moreau-Yosida envelope of  $\delta_{\mathcal{E}}(\mathbf{x}, \alpha)$

is  $\frac{1}{2\lambda}d_{\mathcal{E}}^2(\mathbf{x}, \alpha)$ , which is jointly differentiable in  $\mathbf{x}$  and  $\alpha$ . Subsequently, we can assign  $\alpha$  a prior to incorporate it into posterior inference. Computing with these priors relies on projection onto epigraphs which we describe next.

Projection onto the epigraph of  $g(\mathbf{x}, \alpha)$  depends on the proximal map of  $g(\mathbf{x}, \alpha)$  (Beck, 2017, Theorem 6.36), namely

$$\mathcal{P}_{\mathcal{E}}(\mathbf{x}, \alpha) = \begin{cases} (\mathbf{x}, \alpha) & g(\mathbf{x}) \leq \alpha \\ (\text{prox}_g^{\lambda^*}(\mathbf{x}), \alpha + \lambda^*) & g(\mathbf{x}) > \alpha \end{cases}, \quad (3)$$

where  $\lambda^*$  is any positive root of the auxiliary function

$$F(\lambda) = g(\text{prox}_g^{\lambda}(\mathbf{x})) - \lambda - \alpha,$$

and can be found using bisection.

### 3 An illustrative case study

To introduce our framework, we first consider a canonical example: the lasso regression (Tibshirani, 1996)

$$\text{minimize } \frac{1}{2}\|\mathbf{y} - \mathbf{X}\boldsymbol{\beta}\|_2^2 + \rho\|\boldsymbol{\beta}\|_1, \quad (4)$$

where  $\mathbf{y} \in \mathbb{R}^n$  is a vector of continuous responses,  $\mathbf{X} \in \mathbb{R}^{n \times p}$  is a design matrix whose  $p$  columns are covariates,  $\boldsymbol{\beta} \in \mathbb{R}^p$  is the vector of regression coefficients that we seek to estimate, and  $\rho$  is a nonnegative regularization strength parameter that trades off model fit with sparsity in our estimate of  $\boldsymbol{\beta}$ . To attack this problem in the ProxMCMC framework, we first write the penalized form (4) in an equivalent constrained form

$$\begin{aligned} & \text{minimize } \frac{1}{2}\|\mathbf{y} - \mathbf{X}\boldsymbol{\beta}\|_2^2 \\ & \text{subject to } \|\boldsymbol{\beta}\|_1 \leq \alpha. \end{aligned}$$

There is a one-to-one correspondence between the regularization strength parameter  $\rho$  and the constraint parameter  $\alpha$ . For this reason we will refer to  $\alpha$  as the regularization strength parameter as well. We specify the following Bayesian hierarchical model for the constrained formulation of the lasso:

- Data likelihood:  $\mathbf{Y} | \boldsymbol{\beta}, \sigma^2 \sim N(\mathbf{X}\boldsymbol{\beta}, \sigma^2\mathbf{I})$ ,
- A prior  $\pi(\sigma^2)$  for the variance:  $\sigma^2 \sim IG(r_{\sigma^2}, s_{\sigma^2})$ , where  $IG(r, s)$  denotes the Inverse-Gamma distribution with scale parameter  $r$  and shape parameter  $s$  (mean =  $\frac{r}{s-1}$  for  $s > 1$ ),
- A prior  $\pi(\boldsymbol{\beta} | \alpha)$  for  $\boldsymbol{\beta}$  conditional on  $\alpha$ , namely

$$\pi(\boldsymbol{\beta} | \alpha) = \frac{p!}{\alpha^{p2^p}} \exp[-\delta_{\mathcal{E}}(\boldsymbol{\beta}, \alpha)],$$

where  $\mathcal{E} = \{(\boldsymbol{\beta}, \alpha) : \|\boldsymbol{\beta}\|_1 \leq \alpha\}$  and  $\frac{p!}{\alpha^{p2^p}}$  is the reciprocal of the volume of  $\mathcal{E}$ . Note that  $\pi(\boldsymbol{\beta} | \alpha)$  is a flat prior over an  $\ell_1$ -ball of radius  $\alpha$ .

- A prior  $\pi(\alpha)$  on  $\alpha$  that controls the  $\ell_1$ -regularization strength:  $\alpha \sim IG(r_\alpha, s_\alpha)$ .

The distribution  $\pi(\boldsymbol{\beta}, \alpha) = \pi(\boldsymbol{\beta} \mid \alpha) \cdot \pi(\alpha)$  specifies a prior on the epigraph  $\mathcal{E} = \{(\boldsymbol{\beta}, \alpha) : \|\boldsymbol{\beta}\|_1 \leq \alpha\} \subset \mathbb{R}^{p+1}$ . The posterior log-density takes the following form, up to an irrelevant additive constant,

$$\begin{aligned} \log \pi(\boldsymbol{\beta}, \sigma^2, \alpha) &= - \left( \frac{n}{2} + s_{\sigma^2} + 1 \right) \log \sigma^2 - \frac{\|\mathbf{y} - \mathbf{X}\boldsymbol{\beta}\|^2 + 2r_{\sigma^2}}{2\sigma^2} \\ &\quad - (s_\alpha + 1) \log \alpha - \frac{r_\alpha}{\alpha} - g(\boldsymbol{\beta}, \alpha), \end{aligned}$$

where  $g(\boldsymbol{\beta}, \alpha) = \delta_{\mathcal{E}}(\boldsymbol{\beta}, \alpha)$ .

The above posterior is not differentiable, but we can approximate it arbitrarily well with a differentiable posterior. The key idea is to approximate the non-smooth function  $g(\boldsymbol{\beta}, \alpha)$  by its Moreau-Yosida envelope  $g^\lambda(\boldsymbol{\beta}, \alpha)$ . The smoothed posterior log-density is

$$\begin{aligned} \log \pi^\lambda(\boldsymbol{\beta}, \sigma^2, \alpha) &= - \left( \frac{n}{2} + s_{\sigma^2} + 1 \right) \log \sigma^2 - \frac{\|\mathbf{y} - \mathbf{X}\boldsymbol{\beta}\|^2 + 2r_{\sigma^2}}{2\sigma^2} \\ &\quad - (s_\alpha + 1) \log \alpha - \frac{r_\alpha}{\alpha} - g^\lambda(\boldsymbol{\beta}, \alpha), \end{aligned}$$

which, due to the smoothness of the Moreau-Yosida envelope  $g^\lambda(\boldsymbol{\beta}, \alpha)$  (Rockafellar and Wets, 2009), can be readily sampled using any of a multitude of sampling algorithms for smooth log-densities. In this paper, we use Hamiltonian Monte Carlo (HMC) (Neal et al., 2011) due to its efficiency and generality. Since HMC works on unconstrained domains, we use the parameterization  $(\boldsymbol{\beta}, \log \sigma^2, \log \alpha)$ , so

$$\begin{aligned} \log \pi^\lambda(\boldsymbol{\beta}, \log \sigma^2, \log \alpha) &= - \left( \frac{n}{2} + s_{\sigma^2} \right) \log \sigma^2 - \frac{\|\mathbf{y} - \mathbf{X}\boldsymbol{\beta}\|^2 + 2r_{\sigma^2}}{2\sigma^2} \\ &\quad - s_\alpha \log \alpha - \frac{r_\alpha}{\alpha} - g^\lambda(\boldsymbol{\beta}, \alpha). \end{aligned}$$

We compare ProxMCMC to the Bayesian lasso on the diabetes data set in Efron et al. (2004). The outcome is a quantitative measure of disease progression over a year, and the covariates are age, sex, body mass index, average blood pressure, and six blood serum measurements. All variables are standardized to have zero mean and unit variance. For the Bayesian lasso, we use the `blasso` function from the R package `monomvn` (Gramacy, 2019) with default parameters. We show the results of the Bayesian lasso with and without using reversible jump MCMC (RJMCMC) to perform model selection. For ProxMCMC, we set  $\lambda = 0.001$ ,  $\sigma^2 \sim IG(0.1, 0.1)$ , and  $\alpha \sim IG(1, 10 + 2)$ . We also calculate the 95% selective inference confidence intervals (Lee et al., 2016) using the R package `selectiveInference` (Tibshirani et al., 2019). Since this method requires a model to be selected first, we use lasso with 10-fold cross-validation and choose the largest regularization parameter such that the error is within 1 standard error of the minimum (the `lambda.1se` option from the `glmnet` package). Figure 2 displays the interval estimates of the regression coefficient computed by each method. We see that for null covariates, the credible intervals of the Bayesian lasso are narrower when model selection by RJMCMC is used. This is because RJMCMC results in many exact zeros (75% in this example) in the posterior sample, which reduce the variability and thus the width of credible intervals. When RJMCMC is not used, the credible intervals of the null covariates become

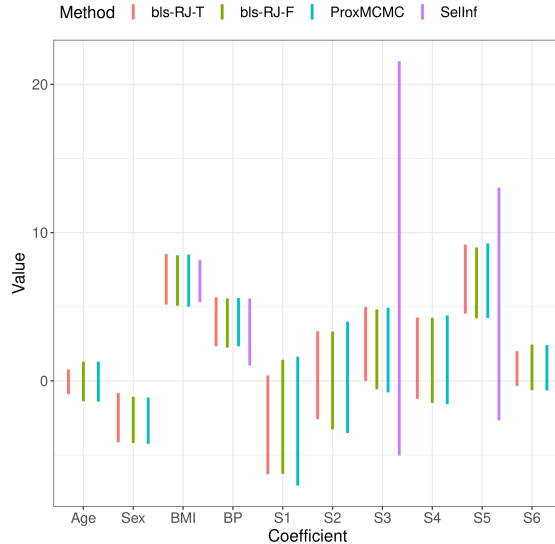


Figure 2: The 95% credible intervals calculated by Bayesian lasso (bls) and ProxMCMC. bls-RJ-T denotes that RJMCMC is used in computing the posterior samples of the Bayesian lasso, while bls-RJ-F denotes results when RJMCMC is not used. Also shown are the 95% selective inference confidence intervals (SelInf) for the four variables selected by the lasso using 10-fold cross-validation.

wider and are similar to those obtained by the ProxMCMC method. The credible intervals for non-null covariates are similar regardless of which method is used. The selective inference confidence intervals have a different interpretation. The coverage guarantee is in the frequentist sense and is conditional on the model being selected, so they are not directly comparable with credible intervals. Nevertheless, it is interesting to note that two of the four intervals for the selected variables are extremely wide.

## 4 Methodology

Having seen how to apply our ProxMCMC method in the special case of the lasso, we next present the framework in greater generality. Our proposed ProxMCMC method consists of three steps.

**1. Likelihood and prior.** The first step is to specify the likelihood model for the data  $Y$  and priors for the model parameters. This is a standard step in Bayesian modeling. For incorporating a penalty function  $g(\mathbf{x})$  with a regularization strength parameter  $\alpha$ , we specify a prior through an indicator function  $\delta_{\mathcal{E}}(\mathbf{x}, \alpha)$  on the epigraph set

$$\mathcal{E} = \{(\mathbf{x}, \alpha) : g(\mathbf{x}) \leq \alpha\}.$$

For example, in the lasso example where  $\boldsymbol{\beta}$  was a vector of regression coefficients and  $\alpha$  was a regularization parameter,  $\mathcal{E} = \{(\boldsymbol{\beta}, \alpha) : \|\boldsymbol{\beta}\|_1 \leq \alpha\}$ .

Note that the regularization parameter  $\alpha$  must be nonnegative and thus requires a prior with nonnegative support. In our experience, placing an inverse Gamma prior on  $\alpha$  works well in practice

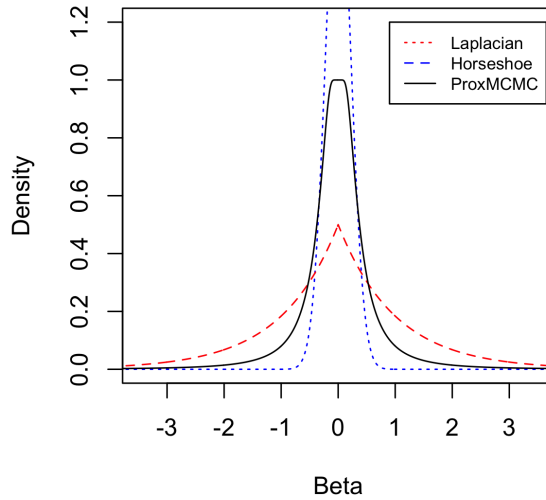


Figure 3: The ProxMCMC epigraph prior and two other commonly used shrinkage priors.

and will be used throughout this paper.

To gain a sense of how the ProxMCMC epigraph prior differs from existing alternatives, consider the simple case where we put a  $\ell_1$ -penalty on a single parameter  $\beta$ , namely

$$\mathcal{E} = \{(\beta, \alpha) : |\beta| \leq \alpha\}.$$

With an  $IG(r, s)$  prior on  $\alpha$ , the marginal density for  $\beta$  is

$$f_{\beta}(t) = \int_{|t|}^{\infty} \frac{1}{2\alpha} \pi(\alpha) d\alpha = \frac{s}{2r} [1 - F_{IG(r, s+1)}(|t|)],$$

where  $F_{IG(r, s+1)}(|t|)$  is the cumulative distribution function of  $IG(r, s + 1)$  evaluated at  $|t|$ . Figure 3 contrasts the prior densities of the ProxMCMC epigraph prior, Laplacian prior, and horseshoe prior. We can see that the ProxMCMC epigraph prior density shrinks small  $\beta$  while allowing strong signals to remain large.

In the multivariate case, when a vector of parameters  $\beta$  is penalized, e.g.,  $\mathcal{E} = \{(\beta, \alpha) : \|\beta\|_1 \leq \alpha\}$ , the ProxMCMC epigraph prior enforces negative correlation among the components of  $\beta$ . This repulsive feature distinguishes it from other Bayesian priors such as the Laplacian or horseshoe prior, where components of  $\beta$  are independent of each other conditional on the hyperparameter and marginally positively correlated.

Besides incorporating penalties, our framework can also handle cases where we wish to impose constraints. As before, we will enforce the constraints via an indicator function of the constraint set.

Once the likelihood model and the priors are specified, we can write down the posterior. Let  $\theta \in \mathbb{R}^d$  denote all model parameters, which includes the constrained or regularized parameters

$\boldsymbol{\tau} \in \mathbb{R}^p$  and all other parameters  $\boldsymbol{\eta} \in \mathbb{R}^q$  (so  $d = p + q$ ) including the regularization strength parameter  $\alpha$ . Further let  $\ell(\boldsymbol{\theta})$  be the log-likelihood,  $\pi(\boldsymbol{\eta})$  denote the prior density for  $\boldsymbol{\eta}$ , and  $g(\boldsymbol{\tau}) = \delta_{\mathcal{E}}(\boldsymbol{\tau})$ , where  $\mathcal{E}$  denotes either the constraint set or the epigraph set depending on the problem. Note that if  $\mathcal{E}$  is an epigraph set, then  $g$  is a function of both  $\boldsymbol{\tau}$  and  $\alpha$ , otherwise it is a function of  $\boldsymbol{\tau}$  alone. For simplicity, we will write  $g(\boldsymbol{\tau})$  unless it is necessary to be more specific. The posterior density is given by

$$\pi(\boldsymbol{\theta} | Y) = \frac{e^{-U(\boldsymbol{\theta})}}{\int e^{-U(\boldsymbol{s})} d\boldsymbol{s}},$$

where  $U(\boldsymbol{\theta}) = f(\boldsymbol{\theta}) + g(\boldsymbol{\tau})$  and  $f(\boldsymbol{\theta}) = -\ell(\boldsymbol{\theta}) - \log \pi(\boldsymbol{\eta})$ . The posterior  $\pi(\boldsymbol{\theta} | Y)$  is not differentiable because  $g(\boldsymbol{\tau})$  is not differentiable, but  $\pi(\boldsymbol{\theta} | Y)$  can be smoothed by substituting  $g(\boldsymbol{\tau})$  with its Moreau-Yosida envelope  $g^\lambda(\boldsymbol{\tau})$  so that both  $U^\lambda(\boldsymbol{\theta}) = f(\boldsymbol{\theta}) + g^\lambda(\boldsymbol{\tau})$  and

$$\pi^\lambda(\boldsymbol{\theta} | Y) = \frac{e^{-U^\lambda(\boldsymbol{\theta})}}{\int e^{-U^\lambda(\boldsymbol{s})} d\boldsymbol{s}}$$

become smooth functions.

**2. Gradient.** We need to efficiently evaluate the gradient of the smoothed posterior log-density. This is another standard step in Bayesian modeling, and for commonly used likelihood models and priors, the gradient can be computed numerically by auto-differentiation in software packages such as `Stan` (Stan Development Team, 2020) and `Turing.jl` (Ge et al., 2018).

As noted earlier, the existence of the gradient of the Moreau-Yosida envelope  $g^\lambda(\boldsymbol{\tau})$  depends on the convexity of  $g(\boldsymbol{\tau})$  and thus of the convexity of the regularization term or constraint set  $\mathcal{E}$ . When  $g(\boldsymbol{\tau})$  is convex, which is the case for many commonly used regularization and constraints, proximal mappings have been extensively studied in the optimization literature (Beck, 2017, Chapter 6) and efficient implementations are available from mature libraries such as FOM Matlab toolbox (Beck and Guttman-Beck, 2019), Python package `PyProximal`, and Julia package `ProximalOperators.jl`.

When  $g(\boldsymbol{\tau})$  is non-convex,  $g^\lambda(\boldsymbol{\tau})$  is no longer differentiable. However, as we will show in Section 5.4, under certain regularity conditions,  $g^\lambda(\boldsymbol{\tau})$  will be semidifferentiable and we can calculate a subgradient using the above formula and use it in place of gradient in gradient based samplers.

**3. Sampling algorithm.** Finally, we invoke a gradient based sampling algorithm such as HMC or the Langevin algorithm to efficiently explore the posterior landscape. Software libraries include `DynamicHMC.jl`, `AdvancedHMC.jl`, and `pyhmc`, to name a few.

**Remark:** Before we proceed to examples, we pause to highlight ProxMCMC’s close connection to distance majorization and proximal distance algorithms (Chi et al., 2014; Xu et al., 2017; Keys et al., 2019; Landeros and Lange, 2021; Landeros et al., 2022b,a). Proximal distance algorithms are used to solve distance penalty problems.

$$\text{minimize } f(\boldsymbol{\theta}) + \frac{\rho}{2} d_{\mathcal{E}}(\boldsymbol{\theta})^2, \tag{5}$$

where  $f(\boldsymbol{\theta})$  is typically a negative log-likelihood term quantifying model fit,  $\mathcal{E}$  is a target constraint set that we wish our estimate of  $\boldsymbol{\theta}$  to be close to, and  $\rho$  is a nonnegative tuning parameter that trades

off model fit with the amount of constraint violation quantified as the distance to  $\mathcal{E}$ . A solution to (5) is a maximum a posteriori estimate under a distance-to-set prior  $\pi(\boldsymbol{\theta}) \propto \exp(-\frac{\rho}{2}d_{\mathcal{E}}(\boldsymbol{\theta})^2)$ . Thus, the ProxMCMC method that we introduce in this work provides a fully Bayesian framework for generating posterior samples under a distance-to-epigraph set prior.

## 5 Examples

We present four examples to illustrate the generality of ProxMCMC. Since the potential applications of ProxMCMC are innumerable, our examples are not comprehensive. Nonetheless, we chose these four examples because inference in these problems are either unknown or regarded difficult.

### 5.1 Constrained lasso

The constrained lasso problem is formulated as

$$\begin{aligned} & \text{minimize} && \frac{1}{2}\|\mathbf{y} - \mathbf{X}\boldsymbol{\beta}\|_2^2 + \rho\|\boldsymbol{\beta}\|_1 \\ & \text{subject to} && \mathbf{A}\boldsymbol{\beta} = \mathbf{b}, \end{aligned}$$

where  $\mathbf{A}$  has full row-rank. The constrained lasso is relevant to the analysis of compositional data, where the rows of  $\mathbf{A}$  represents proportions of a whole and thus must sum to one. The method has been applied in problems involving consumer spending in economics, topic consumption of documents in machine learning, and the analysis of the human microbiome (Gaines et al., 2018; James et al., 2020).

The  $\ell_1$ -penalization is reparameterized using an indicator function on the epigraph of the  $\ell_1$ -norm

$$\mathcal{E}_1 = \{(\boldsymbol{\beta}, \alpha) : \|\boldsymbol{\beta}\|_1 \leq \alpha\}.$$

The equality constraint is imposed through an indicator function on the hyperplane

$$\mathcal{E}_2 = \{\boldsymbol{\beta} : \mathbf{A}\boldsymbol{\beta} = \mathbf{b}\}.$$

We use an  $IG(r_{\sigma^2}, s_{\sigma^2})$  prior for  $\sigma^2$  and an  $IG(r_{\alpha}, s_{\alpha})$  prior for  $\alpha$ . Using the  $(\boldsymbol{\beta}, \log \sigma^2, \log \alpha)$  parameterization, the smoothed posterior log-density up to an irrelevant additive constant is

$$\begin{aligned} \log \pi^{\lambda}(\boldsymbol{\beta}, \log \sigma^2, \log \alpha) = & -\left(\frac{n}{2} + s_{\sigma^2}\right) \log \sigma^2 - \frac{\|\mathbf{y} - \mathbf{X}\boldsymbol{\beta}\|_2^2 + 2r_{\sigma^2}}{2\sigma^2} \\ & - s_{\alpha} \log \alpha - \frac{r_{\alpha}}{\alpha} - g_1^{\lambda}(\boldsymbol{\beta}, \alpha) - g_2^{\lambda}(\boldsymbol{\beta}), \end{aligned}$$

where  $g_1^{\lambda}(\boldsymbol{\beta}, \alpha)$  and  $g_2^{\lambda}(\boldsymbol{\beta})$  are the Moreau-Yosida envelopes of the indicator functions  $g_1(\boldsymbol{\beta}, \alpha) = \delta_{\mathcal{E}_1}(\boldsymbol{\beta}, \alpha)$  and  $g_2(\boldsymbol{\beta}) = \delta_{\mathcal{E}_2}(\boldsymbol{\beta})$ , respectively. According to (3), the proximal map of  $g_1(\boldsymbol{\beta}, \alpha)$  is the projection onto the epigraph  $\mathcal{E}_1$

$$\text{prox}_{g_1}^{\lambda}(\boldsymbol{\beta}, \alpha) = \begin{cases} (\boldsymbol{\beta}, \alpha) & \text{if } \|\boldsymbol{\beta}\|_1 \leq \alpha \\ (S_{\lambda^*}(\boldsymbol{\beta}), \alpha + \lambda^*) & \text{if } \|\boldsymbol{\beta}\|_1 > \alpha \end{cases},$$

where  $S_\lambda$  is the soft-thresholding operator given in (2) and  $\lambda^*$  is any positive root of the nonincreasing function  $\phi(\lambda) = \|S_\lambda(\boldsymbol{\beta})\|_1 - \lambda - \alpha$  (Beck, 2017). The proximal map of  $g_2$  is the projection onto the hyperplane given by

$$\text{prox}_{g_2}(\boldsymbol{\beta}) = \boldsymbol{\beta} - \mathbf{A}^T(\mathbf{A}\mathbf{A}^T)^{-1}(\mathbf{A}\boldsymbol{\beta} - \mathbf{b}),$$

assuming  $\mathbf{A}$  has full row rank. The gradient of the posterior log-density is given block-wise by

$$\begin{aligned} \frac{\partial \log \pi^\lambda}{\partial \boldsymbol{\beta}} &= \sigma^{-2} \mathbf{X}^T(\mathbf{y} - \mathbf{X}\boldsymbol{\beta}) - \lambda^{-1} \left[ \boldsymbol{\beta} - \text{prox}_{g_1}^\lambda(\boldsymbol{\beta}, \alpha) \boldsymbol{\beta} \right] \\ &\quad - \lambda^{-1} \left[ \boldsymbol{\beta} - \text{prox}_{g_2}^\lambda(\boldsymbol{\beta}) \right] \\ \frac{\partial \log \pi^\lambda}{\partial \log \sigma^2} &= -\left(\frac{n}{2} + s_{\sigma^2}\right) + \frac{\|\mathbf{y} - \mathbf{X}\boldsymbol{\beta}\|^2 + 2r_{\sigma^2}}{2\sigma^2} \\ \frac{\partial \log \pi^\lambda}{\partial \log \alpha} &= -s_\alpha + \frac{r_\alpha}{\alpha} - \lambda^{-1} \alpha [\alpha - \text{prox}_g^\lambda(\boldsymbol{\beta}, \alpha)]_\alpha. \end{aligned}$$

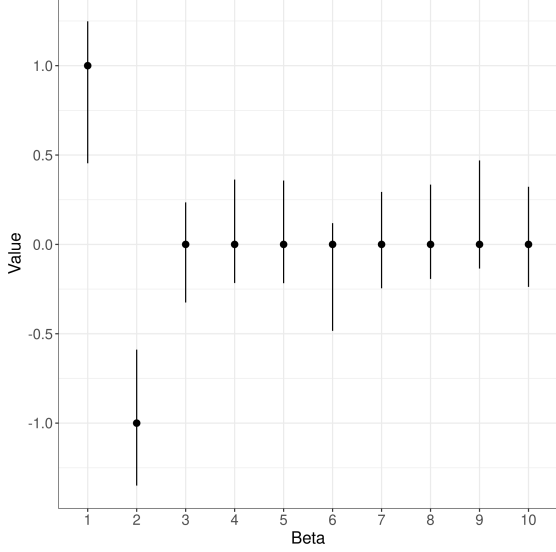
### 5.1.1 Simulated microbiome data

We illustrate our proxMCMC method for the constrained lasso using a simulated microbiome data set. The 16S microbiome sequencing technology measures the number of various organisms called operational taxonomic units (OTUs) in samples. For statistical analysis, counts are normalized into proportions for each sample, resulting in a covariate matrix  $\mathbf{X}$  with each of its rows summing to 1. For identifiability, we need to have a sum-to-zero constraint on the regression coefficients, i.e.,  $\sum_j \beta_j = 0$ . We generate a data set with  $n = 300$  samples and  $p = 20$  OTUs. We set  $\beta_1 = 1$ ,  $\beta_2 = -1$  and the remaining  $\beta_j$ ,  $j = 3, \dots, 20$ , to 0 so that 10% of the entries in  $\boldsymbol{\beta}$  are nonzero. The design matrix  $\mathbf{X}$  is generated as follows. First, for each element in  $\mathbf{X}$  an i.i.d. sample from a uniform distribution ( $U_{[0,1]}$ ) is drawn. Second, the rows of  $\mathbf{X}$  are then scaled so that each row of  $\mathbf{X}$  sums to 1. The noise is generated from a normal distribution with mean 0 and  $\sigma = 0.1$  so that the sample signal-to-noise ratio  $\text{Var}(\mathbf{X}\boldsymbol{\beta})/\sigma^2$  is approximately 0.2. We use  $IG(0.1, 0.1)$  as a prior for  $\sigma^2$  and  $IG(1, p+1)$  as a prior for  $\alpha$ , set  $\lambda = 10^{-6}$ , and ran HMC for 10,000 iterations. From Figure 4 (a), we can see that the 95% credible intervals provide good coverage for the first 10 coefficients; those for the other coefficients are similar. Figure 4 (b) shows the histogram of posterior samples of  $\sum_j \beta_j$ , which is highly concentrated around 0.

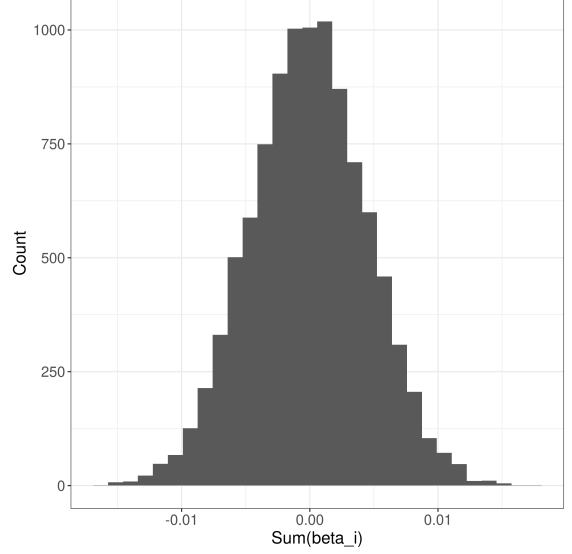
## 5.2 Graphical lasso

Given i.i.d.  $p$ -dimensional observations  $\{\mathbf{x}_1, \dots, \mathbf{x}_n\}$ , where  $\mathbf{x}_i \sim N(\mathbf{0}, \boldsymbol{\Sigma})$ , the graphical lasso method infers the underlying conditional dependencies among the covariates by estimating the precision matrix  $\boldsymbol{\Theta} = \boldsymbol{\Sigma}^{-1}$  through maximizing the regularized log-likelihood

$$-\frac{n}{2} \text{tr}(\mathbf{S}\boldsymbol{\Theta}) + \frac{n}{2} \log \det(\boldsymbol{\Theta}) - \rho \sum_{j \neq k} |\boldsymbol{\Theta}_{jk}|,$$



(a) 95% credible intervals for the first 10 coefficients. Dots mark the truth.



(b) Histogram of  $\sum_i \beta_i$ .

Figure 4: Results from the simulated microbiome data

where  $\mathbf{S}$  is the sample covariance and  $\rho$  is the regularization strength parameter. Equivalently, we can maximize

$$-\frac{n}{2} \text{tr}(\mathbf{S}\mathbf{\Theta}) + \frac{n}{2} \log \det(\mathbf{\Theta}) - g(\mathbf{\Theta}, \alpha),$$

where  $g(\mathbf{\Theta}, \alpha) = \delta_{\mathcal{E}}(\mathbf{\Theta}, \alpha)$  and  $\mathcal{E} = \{(\mathbf{\Theta}, \alpha) : \sum_{j \neq k} |\mathbf{\Theta}_{jk}| \leq \alpha\}$ . The function  $g(\mathbf{\Theta}, \alpha)$  can be thought as a uniform prior for  $\mathbf{\Theta}$  over the  $\ell_1$ -ball  $\{\mathbf{\Theta} : \sum_{j \neq k} |\mathbf{\Theta}_{jk}| \leq \alpha\}$ . With an  $IG(r_\alpha, s_\alpha)$  prior for  $\alpha$ , the smoothed posterior log-density of  $(\mathbf{\Theta}, \log \alpha)$  is

$$\begin{aligned} \log \pi^\lambda(\mathbf{\Theta}, \log \alpha) &= -\frac{n}{2} \text{tr}(\mathbf{S}\mathbf{\Theta}) + \frac{n}{2} \log \det(\mathbf{\Theta}) \\ &\quad - s_\alpha \log \alpha - \frac{r_\alpha}{\alpha} - g^\lambda(\mathbf{\Theta}, \alpha). \end{aligned}$$

Since HMC works on unconstrained domains and  $\mathbf{\Theta}$  needs to be positive definite, we parameterize  $\mathbf{\Theta}$  in terms of its lower Cholesky factor  $\mathbf{L}$ . Adjusting for the log-Jacobian terms, the smoothed posterior log-density becomes

$$\begin{aligned} \log \pi^\lambda(\mathbf{L}, \log \alpha) &= -\frac{n}{2} \text{tr}(\mathbf{S}\mathbf{L}\mathbf{L}^T) + \frac{n}{2} \log \det(\mathbf{L}\mathbf{L}^T) \\ &\quad - s_\alpha \log \alpha - \frac{r_\alpha}{\alpha} - g^\lambda(\mathbf{L}\mathbf{L}^T, \alpha) \\ &\quad + p \log(2) + \sum_{j=1}^p (p - j + 2) \mathbf{L}_{jj}. \end{aligned}$$

The gradients are given by

$$\begin{aligned} \nabla_{\text{vech } \mathbf{L}} \log \pi^\lambda &= -(n \text{vech}(\mathbf{S}\mathbf{L}))^T + n(\text{vech}(\mathbf{L}^{-1})^T)^T \\ &\quad - \frac{2}{\lambda} \left( \text{vech} \left( [\mathbf{\Theta} - \text{prox}_g^\lambda(\mathbf{\Theta}, \alpha) \mathbf{\Theta}] \mathbf{L} \right) \right)^T \\ &\quad + \left( \text{vech}(\text{diag}(p+1, p, \dots, 2)) \right)^T \\ \frac{\partial \log \pi^\lambda}{\partial \log \alpha} &= -s_\alpha + \frac{r_\alpha}{\alpha} - \lambda^{-1} \alpha [\alpha - \text{prox}_g^\lambda(\mathbf{\Theta}, \alpha)_\alpha], \end{aligned}$$

where  $\text{vech}(\mathbf{A})$  denotes the vector obtained from stacking the columns of the lower triangular part of a square matrix  $\mathbf{A}$ .

### 5.2.1 Cytometry data

We compare ProxMCMC with the Bayesian graphical lasso (Wang, 2012) on the cell-signalling data from Sachs et al. (2005), which was used in the original graphical lasso paper (Friedman et al., 2008). The data set contains flow cytometry measurements on  $p = 11$  proteins and  $n = 7466$  cells. We first use the R package `CVglasso` to compute 5-fold cross-validated graphical lasso estimates for  $\mathbf{\Theta}$  and use them as reference in the results below. For the Bayesian graphical lasso we use the R package `BayesianGLasso` (Wang, 2012). We experimented with both the default prior and a few other prior settings, but found little difference among them. Thus we report the results using the default prior (Gamma distribution with shape parameter 1 and scale parameter 0.1). For ProxMCMC we use an  $IG(1, p+1)$  prior for  $\alpha$  and set  $\lambda = 0.01$ . We ran 10,000 iterations for both methods. Figure 5 displays the credible intervals. Due to the large number of parameters, we only show the results for the first ten parameters in the plot, but the same pattern is observed in other parameters. We can see that the ProxMCMC credible intervals are consistently narrower and provide good coverage of the graphical lasso estimate, whereas those provided by the Bayesian graphical lasso can be wide and fail to cover the cross-validated estimates. Among all 66 parameters, all ProxMCMC credible intervals cover the reference values whereas only 24% of the Bayesian graphical lasso credible intervals do.

### 5.3 Matrix completion

Given a matrix  $\mathbf{Y}$  with entries only observed on the set  $\Omega = \{(i, j) : y_{ij} \text{ is observed}\}$ , Mazumder et al. (2010) propose to complete the matrix by minimizing the convex objective function

$$\frac{1}{2} \sum_{(i,j) \in \Omega} (y_{ij} - x_{ij})^2 + \rho \|\mathbf{X}\|_*,$$

where  $\rho$  is a regularization strength parameter and  $\|\mathbf{X}\|_*$  is the nuclear norm of the completed matrix  $\mathbf{X}$ . The nuclear norm is defined as  $\|\mathbf{X}\|_* = \|\boldsymbol{\sigma}(\mathbf{X})\|_1 = \sum_i \sigma_i(\mathbf{X})$ , where  $\sigma_1(\mathbf{X}) \geq \dots \geq \sigma_m(\mathbf{X}) \geq 0$  are the singular values of  $\mathbf{X}$ . To put the problem into the ProxMCMC framework, we assume  $\text{vec } \mathbf{Y} \sim N(\text{vec } \mathbf{X}, \sigma^2 \mathbf{I})$ . Let  $\mathcal{E} = \{(\mathbf{X}, \alpha) : \|\mathbf{X}\|_* \leq \alpha\}$  and  $g(\mathbf{X}, \alpha) = \delta_{\mathcal{E}}(\mathbf{X}, \alpha)$ . With an

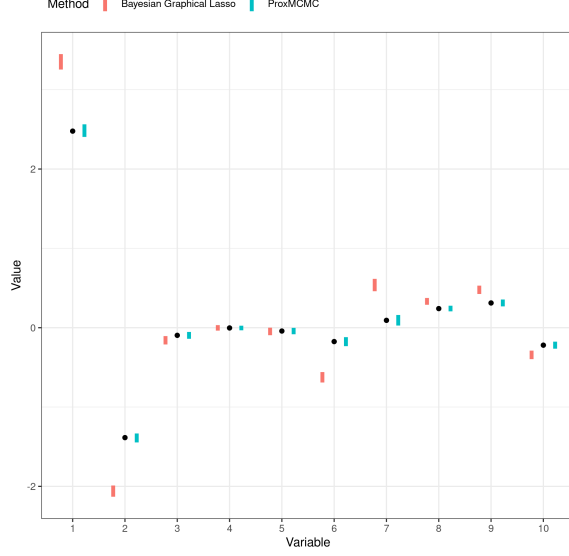


Figure 5: Comparing the 95% credible intervals of Bayesian graphical lasso versus ProxMCMC on the cytometry data. Black dots are estimates obtained from 5-fold cross-validated graphical lasso.

$IG(r_{\sigma^2}, s_{\sigma^2})$  prior for  $\sigma^2$  and an  $IG(r_\alpha, s_\alpha)$  prior for  $\alpha$ , the smoothed posterior log-density using the  $\log \sigma^2, \log \alpha$  parameterization is

$$\begin{aligned} \log \pi^\lambda(\mathbf{X}, \log \sigma^2, \log \alpha) = & - \left( \frac{|\Omega|}{2} + s_{\sigma^2} \right) \log \sigma^2 - \frac{\sum_{(i,j) \in \Omega} (y_{ij} - x_{ij})^2 + 2r_{\sigma^2}}{2\sigma^2} \\ & - s_\alpha \log \alpha - \frac{r_\alpha}{\alpha} - g^\lambda(\mathbf{X}, \alpha), \end{aligned}$$

The proximal mapping of  $g(\mathbf{X}, \alpha)$  is the projection given by

$$\text{prox}_g^\lambda(\mathbf{X}, \alpha) = \begin{cases} (\mathbf{X}, \alpha) & \text{if } \|\mathbf{X}\|_* \leq \alpha \\ (\mathbf{U} \text{diag}(S_{\lambda^*}(\sigma(\mathbf{X}))) \mathbf{V}^T, \alpha + \lambda^*) & \text{if } \|\mathbf{X}\|_* > \alpha \end{cases},$$

where  $S_\lambda$  is the soft-thresholding operator defined in (2) and  $\lambda^*$  is any positive root of the nonincreasing function  $\phi(\lambda) = \|S_\lambda(\sigma(\mathbf{X}))\|_1 - \lambda - \alpha$ . The gradient of the smoothed posterior log-density is

$$\begin{aligned} \frac{\partial \log \pi^\lambda}{\partial \mathbf{X}} &= \sigma^{-2} [P_\Omega(\mathbf{Y}) - P_\Omega(\mathbf{X})] - \lambda^{-1} [\mathbf{X} - \text{prox}_g^\lambda(\mathbf{X}, \alpha) \mathbf{X}], \\ \frac{\partial \log \pi^\lambda}{\partial \log \sigma^2} &= - \left( \frac{|\Omega|}{2} + s_{\sigma^2} \right) + \frac{\sum_{(i,j) \in \Omega} (y_{ij} - x_{ij})^2 + 2r_{\sigma^2}}{2\sigma^2}, \\ \frac{\partial \log \pi^\lambda}{\partial \log \alpha} &= -s_\alpha + \frac{r_\alpha}{\alpha} - \lambda^{-1} \alpha \left[ \alpha - \text{prox}_g^\lambda(\mathbf{X}, \alpha)_\alpha \right], \end{aligned}$$

where  $P_\Omega(\mathbf{Y})$  is the projection of  $\mathbf{Y}$  onto the set of observed entries  $\Omega$ , namely, the  $ij$ -th entry of  $P_\Omega(\mathbf{Y})_{ij}$  is  $y_{ij}$  for  $(i, j) \in \Omega$  and is zero otherwise. Thus, the difference  $P_\Omega(\mathbf{Y}) - P_\Omega(\mathbf{X})$  denotes the matrix of residuals of the observed entries.

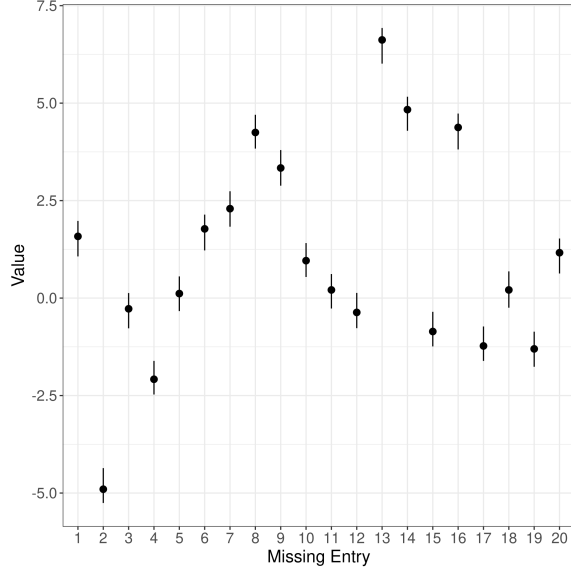


Figure 6: 95% credible intervals and truth (dots) for the first 20 missing entries of the simulated matrix.

### 5.3.1 Simulated matrix

We apply our method to a simulated matrix of size  $250 \times 200$ . The truth is generated by  $\mathbf{Y} = \mathbf{Y}_1 \mathbf{Y}_2 + \sigma \mathbf{E}$  where  $\mathbf{Y}_1$  ( $250 \times 3$ ),  $\mathbf{Y}_2$  ( $3 \times 200$ ), and entries of  $\mathbf{E}$  are generated from the standard normal distribution and  $\sigma = 0.1$ . We randomly mask 20% of the entries (9853 missing) and apply ProxMCMC to calculate 95% credible intervals for the missing entries. We use an  $IG(0.01, 0.01)$  prior for  $\sigma^2$  and an  $IG(1, 250 \times 200 + 1)$  prior for  $\alpha$ , and set  $\lambda = 0.001$ . Figure 6 shows the 95% credible intervals for the first 20 missing entries and we observe that the credible intervals cover the truth well. In fact, all 9853 missing entries are covered by their credible intervals.

## 5.4 Sparse low rank matrix regression

We consider linear regression with matrix covariates, where the rank of coefficient matrix is subject to regularization. One approach is to penalize the nuclear norm of the coefficient matrix (Zhou and Li, 2014), the ProxMCMC version of which is very similar to the matrix completion example above because they share the same proximal map. Alternatively, one can constrain the coefficient matrix to have a user-specified rank  $k$  (Zhou et al., 2013). Here we explore the second approach to illustrate the potential of ProxMCMC for problems where the regularization or constraints are not convex.

Let  $y_i$  be the response for the  $i$ -th sample. Further let  $\mathbf{Z}_i \in \mathbb{R}^p$  and  $\mathbf{X}_i \in \mathbb{R}^{q \times r}$  be the vector and matrix covariates, respectively. The model is

$$y_i = \mathbf{Z}_i^T \boldsymbol{\gamma} + \langle \mathbf{B}, \mathbf{X}_i \rangle + \epsilon_i,$$

where  $\boldsymbol{\gamma}$  and  $\mathbf{B}$  are the vector and matrix coefficients,  $\langle \mathbf{B}, \mathbf{X}_i \rangle = \text{tr}(\mathbf{B}^T \mathbf{X}_i) = \langle \text{vec } \mathbf{B}, \text{vec } \mathbf{X}_i \rangle$  is

the inner product of the two matrices, and  $\epsilon_i \sim N(0, \sigma^2)$ . We fix  $\text{rank}(\mathbf{B})$  at a user-specified value  $k$  through an explicit constraint  $\delta_{\mathcal{E}_1}(\mathbf{B})$  where  $\mathcal{E}_1 = \{\mathbf{B} : \text{rank}(\mathbf{B}) = k\}$ . To promote sparsity in  $\mathbf{B}$ , we also incorporate  $\delta_{\mathcal{E}_2}(\mathbf{B}, \alpha)$ , where  $\mathcal{E}_2 = \{(\mathbf{B}, \alpha) : \|\text{vec } \mathbf{B}\|_1 \leq \alpha\}$ . With a flat prior on  $\gamma$  (i.e.,  $\pi(\gamma) \propto 1$ ), an  $IG(r_{\sigma^2}, s_{\sigma^2})$  prior for  $\sigma^2$ , and an  $IG(r_\alpha, s_\alpha)$  prior for  $\alpha$ , the smoothed posterior log-density is

$$\begin{aligned} \log \pi(\gamma, \mathbf{B}, \log \sigma^2, \log \alpha) = & - \frac{\sum_{i=1}^n (y_i - \mathbf{Z}_i^T \gamma - \langle \mathbf{B}, \mathbf{X}_i \rangle)^2 + 2r_{\sigma^2}}{2\sigma^2} \\ & - \left(\frac{n}{2} + s_{\sigma^2}\right) \log \sigma^2 - s_\alpha \log \alpha - \frac{r_\alpha}{\alpha} \\ & - g_1^\lambda(\mathbf{B}) - g_2^\lambda(\mathbf{B}, \alpha), \end{aligned}$$

where  $g_1^\lambda(\mathbf{B})$  and  $g_2^\lambda(\mathbf{B}, \alpha)$  are the Moreau-Yosida envelopes of  $g_1(\mathbf{B}) = \delta_{\mathcal{E}_1}(\mathbf{B})$  and  $g_2(\mathbf{B}, \alpha) = \delta_{\mathcal{E}_2}(\mathbf{B}, \alpha)$ . The proximal map of  $g_1(\mathbf{B})$  is the projection onto the set  $\mathcal{E}_1$  obtained by thresholding the singular values of  $\mathbf{B}$ . However, since  $g_1^\lambda(\mathbf{B})$  is non-convex, the gradient formula (1) for Moreau-Yosida envelope no longer holds. Instead, we resort to the subsmoothness property of Moreau-Yosida envelopes, for which we need the following definitions (Rockafellar and Wets, 2009).

**Definition 3. (Prox-boundedness)** A function  $g : \mathbb{R}^n \rightarrow \bar{\mathbb{R}}$  is prox-bounded if there exists  $\lambda > 0$  such that its Moreau-Yosida envelope  $g^\lambda > -\infty$  for some  $\mathbf{x} \in \mathbb{R}^n$ . The supremum of the set of all such  $\lambda$  is the threshold  $\lambda_g$  of prox-boundedness for  $g$ .

In the ProxMCMC framework, we only need the Moreau-Yosida envelope of indicator functions, for which we have  $g^\lambda(\mathbf{x}) > -\infty$  for any  $\lambda > 0$ , so they are always prox-bounded and the threshold  $\lambda_g = \infty$ .

**Definition 4. (Semidifferentiability)** Let  $g : \mathbb{R}^n \rightarrow \bar{\mathbb{R}}$  and  $\bar{\mathbf{x}}$  be a point such that  $g(\bar{\mathbf{x}})$  is finite. If the (possibly infinite) limit

$$\lim_{\tau \downarrow 0, \mathbf{w}' \rightarrow \mathbf{w}} \frac{g(\bar{\mathbf{x}} + \tau \mathbf{w}') - g(\bar{\mathbf{x}})}{\tau}$$

exists, it is the semiderivative of  $g$  at  $\bar{\mathbf{x}}$  for  $\mathbf{w}$ , and  $g$  is semidifferentiable at  $\bar{\mathbf{x}}$  for  $\mathbf{w}$ . If this holds for every  $\mathbf{w}$ ,  $g$  is semidifferentiable at  $\bar{\mathbf{x}}$ .

By Rockafellar and Wets (2009, Example 10.32), if  $g(\mathbf{x})$  is lower-semicontinuous, proper, and prox-bounded with threshold  $\lambda_g$ , then for  $\lambda \in (0, \lambda_g)$ , the Moreau-Yosida envelope  $g^\lambda(\mathbf{x})$  is semidifferentiable and the subgradient set is

$$\partial g^\lambda(\mathbf{x}) \subset \lambda^{-1} \left[ \mathbf{x} - \text{prox}_g^\lambda(\mathbf{x}) \right].$$

The function  $g_1(\mathbf{B}) = \delta_{\mathcal{E}_1}(\mathbf{B})$  satisfies the above conditions, so we can calculate its subgradient

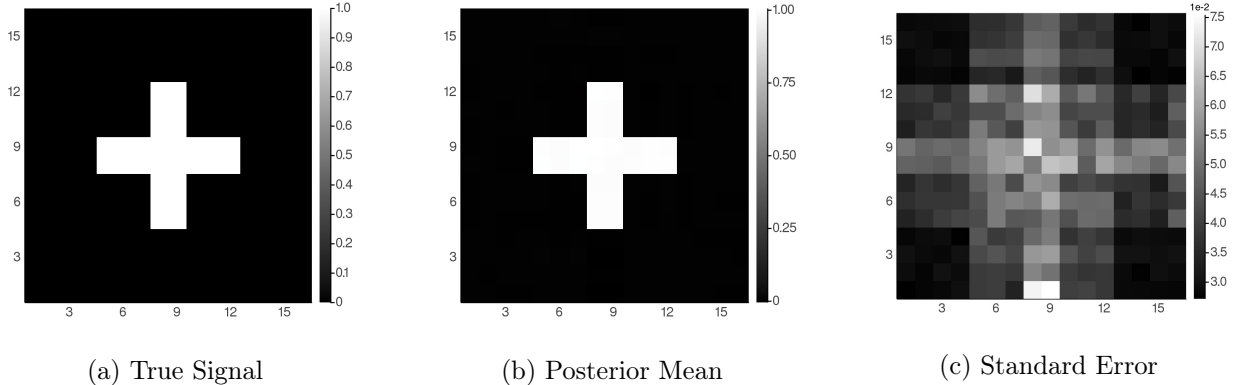


Figure 7: Proximal MCMC for sparse low rank matrix regression on the cross-shaped data.

using the above formula and use it in place of the gradient in HMC

$$\begin{aligned}
\frac{\partial \log \pi}{\partial \boldsymbol{\gamma}} &= \sigma^{-2} \sum_i (y_i - \mathbf{Z}_i^T \boldsymbol{\gamma} - \langle \mathbf{B}, \mathbf{X}_i \rangle) \mathbf{Z}_i, \\
\frac{\partial \log \pi}{\partial \mathbf{B}} &= \sigma^{-2} \sum_i (y_i - \mathbf{Z}_i^T \boldsymbol{\gamma} - \langle \mathbf{B}, \mathbf{X}_i \rangle) \mathbf{X}_i - \lambda^{-1} \left[ \mathbf{B} - \text{prox}_{g_1}^\lambda(\mathbf{B}) \right] \\
&\quad - \lambda^{-1} \left[ \mathbf{B} - \text{prox}_{g_2}^\lambda(\mathbf{B}, \alpha)_{\mathbf{B}} \right], \\
\frac{\partial \log \pi}{\partial \log \sigma^2} &= -\left( \frac{n}{2} + s_{\sigma^2} \right) + \frac{\sum_{i=1}^n (y_i - \mathbf{Z}_i^T \boldsymbol{\gamma} - \langle \mathbf{B}, \mathbf{X}_i \rangle)^2 + 2r_{\sigma^2}}{2\sigma^2}, \\
\frac{\partial \log \pi}{\partial \log \alpha} &= -s_\alpha + \frac{r_\alpha}{\alpha} - \lambda^{-1} \alpha \left[ \alpha - \text{prox}_{g_2}^\lambda(\mathbf{B}, \alpha)_\alpha \right].
\end{aligned}$$

Since  $g_1^\lambda(\mathbf{B})$  is non-convex,  $\text{prox}_{g_1}^\lambda(\mathbf{B})$  is not unique. Our approach is to pick an arbitrary element in the proximal map set, which works well in practice.

#### 5.4.1 Detecting the cross-shaped signal

We illustrate the method on a simulated data of cross-shaped signal. The mean responses are  $\mu_i = \mathbf{Z}_i^T \boldsymbol{\gamma} + \langle \mathbf{B}, \mathbf{X}_i \rangle$ , where  $\mathbf{Z}_i \in \mathbb{R}^2$  and  $\mathbf{X}_i \in \mathbb{R}^{16 \times 16}$  and their entries are generated from i.i.d. standard normal. We set  $\boldsymbol{\gamma} = (1, 1)^T$  and  $\mathbf{B}$  to have a cross shape (Figure 7(a)), where the white cross entries equal 1 and the rest 0. The response  $y_i$  equals  $\mu_i + \epsilon_i$ , where  $\epsilon_i$  ( $i = 1, \dots, n$  and  $n = 100$ ) are also generated from independent standard normal. We use an  $IG(0.01, 0.01)$  prior for  $\sigma^2$  and an  $IG(\sum_i \sigma(\mathbf{B}_0)_i, 2)$  prior for  $\alpha$ , where  $\sigma(\mathbf{B}_0)_i$  is the  $i$ -th singular value of  $\mathbf{B}_0$  and  $\mathbf{B}_0$  is the initial estimate of  $\mathbf{B}$  obtained by least squares without regularization or constraints. We set the Moreau-Yosida envelope parameter  $\lambda = 0.001$ . Figure 7 shows the true signal  $\mathbf{B}$  (panel (a)), the posterior mean from 10,000 HMC samples (panel (b)), and the standard error (panel (c)). Due to space limitations, we only show the 95% credible intervals of the 8-th column of  $\mathbf{B}$  (Figure 8), but all entries of  $\mathbf{B}$  are covered by their 95% credible intervals.

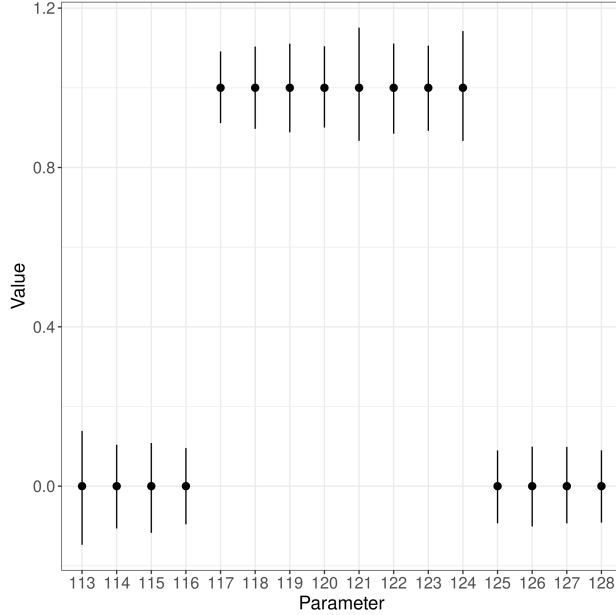


Figure 8: 95% credible intervals of the eighth column of the cross-shaped signal. X-axis indicates their position in  $\text{vec}(\mathbf{B})$ . Dots mark the truth.

## 6 Theoretical properties

This section presents theoretical results for the ProxMCMC method. The proofs simplify those in Durmus et al. (2018) because we focus on the Moreau-Yosida envelope of indicator functions. Our proofs, however, extend to non-convex settings while Durmus et al. (2018) assume convexity. As defined in Section 4,  $\boldsymbol{\theta} \in \mathbb{R}^d$  represents all model parameters that include both the constrained or regularized parameters  $\boldsymbol{\tau} \in \mathbb{R}^p$  and other parameters  $\boldsymbol{\eta} \in \mathbb{R}^q$ . We also use  $\ell(\boldsymbol{\theta})$  for the log-likelihood and  $\pi(\boldsymbol{\eta})$  for the prior density of  $\boldsymbol{\eta}$ . Our main theoretical results are summarized as follows:

**Proposition 1.** (1) For any  $\lambda > 0$ , the smoothed posterior  $\pi^\lambda(\boldsymbol{\theta} | Y)$  defines a proper density of a probability measure on  $\mathbb{R}^d$ , so

$$0 < \int_{\mathbb{R}^d} e^{-U^\lambda(\boldsymbol{\theta})} d\boldsymbol{\theta} < \infty.$$

(2) The approximation  $\pi^\lambda(\boldsymbol{\theta} | Y)$  converges to  $\pi(\boldsymbol{\theta} | Y)$  in total-variation as  $\lambda \downarrow 0$ , i.e.,

$$\lim_{\lambda \downarrow 0} \|\pi^\lambda(\boldsymbol{\theta} | Y) - \pi(\boldsymbol{\theta} | Y)\|_{TV} = 0.$$

*Proof.* (Posterior properness) The properness of the smoothed posterior  $\pi^\lambda(\boldsymbol{\theta} | Y)$  follows from the fact that the Moreau-Yosida envelope of an indicator function is always nonnegative. Specifically, when  $g = \delta_{\mathcal{E}}(\boldsymbol{\tau})$ ,

$$g^\lambda(\boldsymbol{\tau}) = \frac{1}{2\lambda} d_{\mathcal{E}}(\boldsymbol{\tau})^2 \geq 0,$$

where  $d_{\mathcal{E}}(\boldsymbol{\tau}) = \inf_{\mathbf{y} \in \mathcal{E}} d(\boldsymbol{\tau}, \mathbf{y})$  is the distance from  $\boldsymbol{\tau}$  to  $\mathcal{E}$ , so  $-U^\lambda(\boldsymbol{\theta}) = -f(\boldsymbol{\theta}) - g^\lambda(\boldsymbol{\tau}) \leq -f(\boldsymbol{\theta})$ , from which we have

$$e^{-U^\lambda(\boldsymbol{\theta})} \leq e^{-f(\boldsymbol{\theta})}.$$

Since  $f(\boldsymbol{\theta}) = -\ell(\boldsymbol{\theta}) - \log \pi(\boldsymbol{\eta})$  and both the likelihood and the priors  $\pi(\boldsymbol{\eta})$  are integrable (note that  $\boldsymbol{\eta}$  does not include constrained parameters), we have the desired result.

(Convergence in total-variation) Let  $c = \int e^{-U(s)} ds$  and  $c_\lambda = \int e^{-U^\lambda(s)} ds$ . Since  $g^\lambda(\mathbf{x})$  uniformly bounds  $g(\mathbf{x})$  from below, i.e.,  $g^\lambda(\mathbf{x}) \leq g(\mathbf{x})$  for all  $\mathbf{x}$  (Rockafellar and Wets, 2009), we have  $U^\lambda(\mathbf{x}) \leq U(\mathbf{x})$  and thus  $c_\lambda \geq c$ . Note that

$$\begin{aligned} \|\pi^\lambda - \pi\|_{\text{TV}} &= \int |\pi^\lambda(\mathbf{x}) - \pi(\mathbf{x})| d\mathbf{x} \\ &= \int_{\pi^\lambda \geq \pi} [\pi^\lambda(\mathbf{x}) - \pi(\mathbf{x})] d\mathbf{x} + \int_{\pi^\lambda < \pi} [\pi(\mathbf{x}) - \pi^\lambda(\mathbf{x})] d\mathbf{x}. \end{aligned}$$

Let  $\mathcal{A}_1 = \{\mathbf{x} : \pi^\lambda \geq \pi\}$  and  $\mathcal{A}_2 = \{\mathbf{x} : \pi^\lambda < \pi\}$ ,

$$\begin{aligned} &\int_{\mathcal{A}_1} [\pi^\lambda(\mathbf{x}) - \pi(\mathbf{x})] d\mathbf{x} \\ &= \int_{\mathcal{A}_1} \pi^\lambda(\mathbf{x}) \left[1 - \frac{\pi(\mathbf{x})}{\pi^\lambda(\mathbf{x})}\right] d\mathbf{x} \\ &= \int_{\mathcal{A}_1} \pi^\lambda(\mathbf{x}) \left[1 - \frac{c_\lambda}{c} e^{g^\lambda(\mathbf{x}) - g(\mathbf{x})}\right] d\mathbf{x} \\ &\leq \int_{\mathcal{A}_1} [\pi^\lambda(\mathbf{x}) - e^{g^\lambda(\mathbf{x}) - g(\mathbf{x})} \pi^\lambda(\mathbf{x})] d\mathbf{x} \\ &\leq 1 - \frac{c}{c_\lambda}, \end{aligned}$$

and

$$\begin{aligned} &\int_{\mathcal{A}_2} [\pi(\mathbf{x}) - \pi^\lambda(\mathbf{x})] d\mathbf{x} \\ &= \int_{\mathcal{A}_2} \pi(\mathbf{x}) \left[1 - \frac{\pi^\lambda(\mathbf{x})}{\pi(\mathbf{x})}\right] d\mathbf{x} \\ &= \int_{\mathcal{A}_2} \pi(\mathbf{x}) \left[1 - \frac{c}{c_\lambda} e^{g(\mathbf{x}) - g^\lambda(\mathbf{x})}\right] d\mathbf{x} \\ &\leq \int_{\mathcal{A}_2} \pi(\mathbf{x}) \left[1 - \frac{c}{c_\lambda}\right] d\mathbf{x} \\ &\leq 1 - \frac{c}{c_\lambda}. \end{aligned}$$

So  $\|\pi^\lambda - \pi\|_{\text{TV}} \leq 2(1 - \frac{c}{c_\lambda})$ . By (Rockafellar and Wets, 2009), when  $g(\mathbf{x})$  is proper, lower-semicontinuous, and prox-bounded with threshold  $\lambda_g > 0$ ,  $g^\lambda(\mathbf{x})$  converges pointwise to  $g(\mathbf{x})$  as  $\lambda \downarrow 0$ . Moreover, since  $g^\lambda(\mathbf{x})$  is pointwise non-decreasing as  $\lambda$  decreases, by the monotone convergence theorem,  $\lim_{\lambda \downarrow 0} c_\lambda = c$ . Thus

$$\lim_{\lambda \downarrow 0} \|\pi^\lambda - \pi\|_{\text{TV}} \leq \lim_{\lambda \downarrow 0} 2 \left(1 - \frac{c}{c_\lambda}\right) = 0.$$

□

## 7 Discussion

Our examples demonstrate that the ProxMCMC method is a highly flexible tool for performing statistical inference on regularized or constrained statistical learning problems. We find that it works well when the regularization or constraints are non-smooth and even non-convex. In addition, by adopting epigraph priors, our method is fully Bayesian, eliminating the need for tuning the regularization parameter.

For the Moreau-Yosida envelope parameter  $\lambda$ , a smaller value leads to better satisfaction of the constraints. For example, the histogram of  $\sum_j \beta_j$  from the microbiome example is more concentrated around 0 when  $\lambda$  is smaller. Extremely small  $\lambda$ , however, renders slow mixing of the sampling algorithm. We recommend using smaller  $\lambda$  when computational resources allow. Setting  $\lambda = 0.001$  works in most applications as the examples show.

Finally, we emphasize that the four examples are meant to whet readers' appetites, not to satiate them. As we mentioned before, the ProxMCMC algorithm is highly modular and can be readily extended to other problems. We hope this paper encourages readers to discover new applications of the ProxMCMC algorithm.

## Funding

This research was partially funded by the grants from National Science Foundation (DMS-2054253) and National Institutes of Health (R35GM141798, R01HG006139).

## References

- Armagan, A., Dunson, D., and Lee, J. (2013). Generalized double Pareto shrinkage. *Statistica Sinica*, 23:119–143.
- Bachoc, F., Preinerstorfer, D., and Steinberger, L. (2020). Uniformly valid confidence intervals post-model-selection. *The Annals of Statistics*, 48(1):440–463.
- Beck, A. (2017). *First-Order Methods in Optimization*, volume 25 of *MOS-SIAM Series on Optimization*. Society for Industrial and Applied Mathematics (SIAM), Philadelphia, PA; Mathematical Optimization Society, Philadelphia, PA.
- Beck, A. and Guttman-Beck, N. (2019). FOM–A MATLAB toolbox of first-order methods for solving convex optimization problems. *Optimization Methods and Software*, 34(1):172–193.
- Berk, R., Brown, L., Buja, A., Zhang, K., and Zhao, L. (2013). Valid post-selection inference. *Ann. Statist.*, 41(2):802–837.
- Bhattacharya, A., Pati, D., Pillai, N. S., and Dunson, D. B. (2015). Dirichlet-Laplace priors for optimal shrinkage. *J. Amer. Statist. Assoc.*, 110(512):1479–1490.

- Carvalho, C. M., Polson, N. G., and Scott, J. G. (2010). The horseshoe estimator for sparse signals. *Biometrika*, 97(2):465–480.
- Chi, E. C., Zhou, H., and Lange, K. (2014). Distance majorization and its applications. *Mathematical Programming*, 146(1):409–436.
- Choi, Y., Taylor, J., and Tibshirani, R. (2017). Selecting the number of principal components: Estimation of the true rank of a noisy matrix. *The Annals of Statistics*, pages 2590–2617.
- Combettes, P. L. and Pesquet, J.-C. (2011). *Proximal Splitting Methods in Signal Processing*, pages 185–212. Springer New York, New York, NY.
- Combettes, P. L. and Wajs, V. R. (2005). Signal recovery by proximal forward-backward splitting. *Multiscale Modeling & Simulation*, 4(4):1168–1200.
- Durmus, A., Moulines, E., and Pereyra, M. (2018). Efficient bayesian computation by proximal markov chain monte carlo: when langevin meets moreau. *SIAM Journal on Imaging Sciences*, 11(1):473–506.
- Efron, B., Hastie, T., Johnstone, I., Tibshirani, R., et al. (2004). Least angle regression. *Annals of Statistics*, 32(2):407–499.
- Friedman, J., Hastie, T., and Tibshirani, R. (2008). Sparse inverse covariance estimation with the graphical lasso. *Biostatistics*, 9(3):432–441.
- Gaines, B. R., Kim, J., and Zhou, H. (2018). Algorithms for fitting the constrained lasso. *Journal of Computational and Graphical Statistics*, 27(4):861–871.
- Ge, H., Xu, K., and Ghahramani, Z. (2018). Turing: A language for flexible probabilistic inference. In *Proceedings of the Twenty-First International Conference on Artificial Intelligence and Statistics*, volume 84 of *Proceedings of Machine Learning Research*, pages 1682–1690. PMLR.
- George, E. I. and McCulloch, R. E. (1993). Variable selection via Gibbs sampling. *Journal of the American Statistical Association*, 88(423):881–889.
- Gramacy, R. B. (2019). *monomvn: Estimation for MVN and Student-t Data with Monotone Missingness*. R package version 1.9-13.
- Griffin, J. E. and Brown, P. J. (2012). Structuring shrinkage: some correlated priors for regression. *Biometrika*, 99(2):481–487.
- Griffin, J. E. and Brown, P. J. (2013). Some priors for sparse regression modelling. *Bayesian Anal.*, 8(3):691–702.
- Hans, C. (2011). Elastic net regression modeling with the orthant normal prior. *Journal of the American Statistical Association*, 106(496):1383–1393.

- Ioannidis, J. P. (2005). Why most published research findings are false. *PLoS Medicine*, 2(8):e124.
- James, G. M., Paulson, C., and Rusmevichientong, P. (2020). Penalized and constrained optimization: an application to high-dimensional website advertising. *J. Amer. Statist. Assoc.*, 115(529):107–122.
- Javanmard, A. and Montanari, A. (2014). Confidence intervals and hypothesis testing for high-dimensional regression. *J. Mach. Learn. Res.*, 15:2869–2909.
- Keys, K. L., Zhou, H., and Lange, K. (2019). Proximal distance algorithms: Theory and practice. *Journal of Machine Learning Research*, 20(66):1–38.
- Kuchibhotla, A. K., Brown, L. D., Buja, A., Cai, J., George, E. I., and Zhao, L. H. (2020). Valid post-selection inference in model-free linear regression. *Ann. Statist.*, 48(5):2953–2981.
- Landeros, A. and Lange, K. (2021). Algorithms for sparse support vector machines. arXiv:2110.07691 [stat.ME].
- Landeros, A., Padilla, O. H. M., Zhou, H., and Lange, K. (2022a). Extensions to the proximal distance method of constrained optimization. arXiv:2009.00801 [math.OC].
- Landeros, A., Wu, T. T., and Lange, K. (2022b). Feature selection for vertex discriminant analysis. arXiv:2203.11168 [stat.CO].
- Lee, J. D., Sun, D. L., Sun, Y., and Taylor, J. E. (2016). Exact post-selection inference, with application to the lasso. *The Annals of Statistics*, 44(3):907–927.
- Mazumder, R., Hastie, T., and Tibshirani, R. (2010). Spectral regularization algorithms for learning large incomplete matrices. *Journal of Machine Learning Research*, 11:2287–2322.
- Mitchell, T. J. and Beauchamp, J. J. (1988). Bayesian variable selection in linear regression. *J. Amer. Statist. Assoc.*, 83(404):1023–1036. With comments by James Berger and C. L. Mallows and with a reply by the authors.
- Neal, R. M. et al. (2011). MCMC using Hamiltonian dynamics. *Handbook of Markov Chain Monte Carlo*, 2(11):2.
- Park, T. and Casella, G. (2008). The Bayesian lasso. *J. Amer. Statist. Assoc.*, 103(482):681–686.
- Pereyra, M. (2016). Proximal markov chain monte carlo algorithms. *Statistics and Computing*, 26(4):745–760.
- Piironen, J. and Vehtari, A. (2017). Sparsity information and regularization in the horseshoe and other shrinkage priors. *Electronic Journal of Statistics*, 11(2):5018–5051.
- Polson, N. G. and Scott, J. G. (2010). Shrink globally, act locally: sparse Bayesian regularization and prediction. In *Bayesian Statistics 9*, pages 501–538. Oxford Univ. Press, Oxford.

- Polson, N. G., Scott, J. G., and Willard, B. T. (2015). Proximal algorithms in statistics and machine learning. *Statistical Science*, 30(4):559–581.
- Rockafellar, R. T. and Wets, R. J.-B. (2009). *Variational Analysis*, volume 317. Springer Science & Business Media.
- Rudin, L. I., Osher, S., and Fatemi, E. (1992). Nonlinear total variation based noise removal algorithms. *Physica D: Nonlinear Phenomena*, 60(1):259–268.
- Sachs, K., Perez, O., Pe’er, D., Lauffenburger, D. A., and Nolan, G. P. (2005). Causal protein-signaling networks derived from multiparameter single-cell data. *Science*, 308(5721):523–529.
- Stan Development Team (2020). Stan modeling language users guide and reference manual.
- Taylor, J. and Tibshirani, R. (2018). Post-selection inference for-penalized likelihood models. *Canadian Journal of Statistics*, 46(1):41–61.
- Tibshirani, R. (1996). Regression shrinkage and selection via the lasso. *J. Roy. Statist. Soc. Ser. B*, 58(1):267–288.
- Tibshirani, R., Tibshirani, R., Taylor, J., Loftus, J., Reid, S., and Markovic, J. (2019). *selectiveInference: Tools for Post-Selection Inference*. R package version 1.2.5.
- van de Geer, S., Bühlmann, P., Ritov, Y., and Dezeure, R. (2014). On asymptotically optimal confidence regions and tests for high-dimensional models. *Ann. Statist.*, 42(3):1166–1202.
- Wang, H. (2012). Bayesian graphical lasso models and efficient posterior computation. *Bayesian Analysis*, 7(4):867–886.
- Xu, J., Chi, E., and Lange, K. (2017). Generalized linear model regression under distance-to-set penalties. In Guyon, I., Luxburg, U. V., Bengio, S., Wallach, H., Fergus, R., Vishwanathan, S., and Garnett, R., editors, *Advances in Neural Information Processing Systems*, volume 30. Curran Associates, Inc.
- Zhang, C.-H. and Zhang, S. S. (2014). Confidence intervals for low dimensional parameters in high dimensional linear models. *J. R. Stat. Soc. Ser. B. Stat. Methodol.*, 76(1):217–242.
- Zhou, H. and Li, L. (2014). Regularized matrix regression. *Journal of the Royal Statistical Society: Series B (Statistical Methodology)*, 76(2):463–483.
- Zhou, H., Li, L., and Zhu, H. (2013). Tensor regression with applications in neuroimaging data analysis. *Journal of the American Statistical Association*, 108:540–552.